IN VITRO COMPARISON OF THE APATITE INDUCING ABILITY OF THREE DIFFERENT SBF SOLUTIONS ON Ti6Al4V

Sahil Jalota, A. Cuneyt Tas, and Sarit B. Bhaduri
School of Materials Science and Engineering,
Clemson University, Clemson, SC 29634, USA

ABSTRACT

Coating of titanium-based biomedical devices with a layer of carbonated, apatitic calcium phosphate (CaP) increases their bone-bonding ability. Synthetic or simulated body fluids (SBF) have the ability of forming apatitic calcium phosphates on the immersed titanium alloys within few days to 2 weeks. Apatite-inducing ability of 5 M NaOH-etched surfaces of Ti6Al4V strips (10 x 10 x 1 mm) were tested by using three different SBF solutions all concentrated by a factor of 1.5. SBF solutions used in this comparative study were i) 4.2 mM HCO_3^- TRIS-HCl buffered SBF (*conventional* SBF or *c*-SBF), ii) 27 mM HCO_3^- TRIS-HCl buffered SBF (*Tas*-SBF), and iii) 27 mM HCO_3^- HEPES-NaOH buffered SBF (*revised* SBF or *r*-SBF). *c*-SBF (4.2 mM HCO_3^-) was quite slow in forming CaP on Ti6Al4V strips after 1 week of soaking at 37°C, whereas *Tas*-SBF of 27 mM HCO_3^- was able to fully coat the immersed samples. Cell viability, protein concentration and cell attachment were tested on the coated Ti6Al4V strips by using mouse osteoblasts (7F2).

INTRODUCTION

SBF solutions are able [1-3] to induce apatitic calcium phosphate formation on metals, ceramics or polymers (with proper surface treatments) immersed in them. SBF solutions, in close resemblance to the original Earle's (EBSS) [4] and Hanks' Balanced Salt Solution (HBSS) [5], were prepared to simulate the ion concentrations of human blood plasma. EBSS, which has 26 mM of HCO_3^- and a Ca/P molar ratio of 1.8, should be considered as a close ancestor of today's SBF solutions [3]. HBSS solution has a Ca/P ratio of 1.62. EBSS and HBSS solutions are derived from the physiological saline first developed by Ringer in 1882 [6]. It was recently reported that HBSS solutions are also able to slowly induce apatite formation on titanium [7], due to its low Ca/P ratio. For mimicking the ion concentrations of human blood plasma, SBF solutions have relatively low Ca^{2+} and HPO_4^{2-} concentrations of 2.5 mM and 1.0 mM, respectively [8]. pH values of SBF solutions were fixed at the physiologic value of 7.4 by using buffers, such as TRIS (*tris-hydroxymethyl-aminomethane*)-HCl [3] or HEPES (*2-(4-(2-hydroxyethyl)-1-piperazinyl)ethane sulphonic acid*)-NaOH [9, 10]. The buffering agent TRIS present in conventional SBF (*c*-SBF) formulations, for instance, was reported [11] to form soluble complexes with several cations, including Ca^{2+}, which further reduces the concentration of free Ca^{2+} ions available for the real time calcium phosphate coating. To the best of our knowledge, this behavior has not yet been reported for HEPES. HCO_3^- concentration in SBF solutions has been between 4.2 mM (equal to that of HBSS) [1] and 27 mM in revisited SBFs [12-14]. *c*-SBF, which was first popularized by Kokubo in 1990 [1], can be regarded as a TRIS/HCl-buffered variant of HBSS, whose Ca/P molar ratio was increased from 1.62 to 2.5. HBSS and *c*-SBF solutions have the same low carbonate ion concentrations (i.e., 4.2 mM). Tas *et al.* [12, 13] was the first in 1999 to raise the carbonate ion concentration in a TRIS-HCl buffered SBF solution to 27 mM, while Bigi *et al.* [9] have been the first to do the same in a HEPES-NaOH buffered SBF solution. Table I summarizes these SBF solutions. Eagle's minimum

Table I Ion concentrations of human plasma and synthetic solutions (*mM*)

	Blood plasma	Ringer[6]	EBSS[4]	HBSS[5]	*c*-SBF[1]	*Tas*-SBF[12]	*Bigi*-SBF[9]	*r*-SBF[10]
Na^+	142.0	130	143.5	142.1	142.0	142.0	141.5	142.0
K^+	5.0	4.0	5.37	5.33	5.0	5.0	5.0	5.0
Ca^{2+}	2.5	1.4	1.8	1.26	2.5	2.5	2.5	2.5
Mg^{2+}	1.5		0.8	0.9	1.5	1.5	1.5	1.5
Cl^-	103.0	109.0	123.5	146.8	147.8	125.0	124.5	103.0
HCO_3^-	27.0		**26.2**	4.2	4.2	**27.0**	**27.0**	**27.0**
HPO_4^{2-}	1.0		1.0	0.78	1.0	1.0	1.0	1.0
SO_4^{2-}	0.5		0.8	0.41	0.5	0.5	0.5	0.5
Ca/P	2.5		1.8	1.62	2.5	2.5	2.5	2.5
Buffer					TRIS	TRIS	HEPES	HEPES
pH	7.4	6.5	7.2-7.6	6.7-6.9	7.4	7.4	7.4	7.4

essential medium (MEM) [15] and Dulbecco's phosphate buffer saline (PBS) [16], which are used in cell culture studies, may also be added to this table.

Dorozhkina *et al.* [17] studied the influence of HCO_3^- concentration in SBF solutions and concluded that "increasing the HCO_3^- concentration in *c*-SBF from 4.2 to 27 mM resulted in the formation of homogeneous and much thicker carbonated apatite layers." The same fact was also reported by Kim *et al.* [14] on PET substrates immersed into *r*-SBF. Dorozhkina *et al.* [17] emphasized that HEPES was rather unstable, in comparison to TRIS, and it easily lost some of the initially present dissolved carbonates. Kokubo *et al.* [10], who developed the HEPES-buffered *r*-SBF recipe, also reported that *r*-SBF would release CO_2 gas from the fluid, causing a decrease in HCO_3^- concentration, and an increase in pH value, when the storage period was long. Furthermore, they clearly stated that *r*-SBF would not be suitable for long-term use in the biomimetic coating processes owing to its instability [10]. To accelerate the SBF-coating processes, solutions equal to 1.5 times the ionic concentration of SBF were often used [2]. The aim in coating otherwise bioinert materials (such as, PET [14] or PTFE [18]) should have been the formation of bonelike, carbonated (not greater than 6 to 8% by weight) calcium phosphate layers with Ca/P molar ratios in the range of 1.55 to 1.67 [19].

The *in vitro* apatite-inducing ability of neither *Tas*-SBF [12] nor *r*-SBF [10] has yet been reported on Ti6Al4V substrates, in direct comparison to *c*-SBF. The motivation for the present study stems from our interest in finding experimental evidence to the following questions: (a) do the use of different buffers (TRIS or HEPES) in SBFs cause remarkable changes in the morphology or thickness of the calcium phosphate coat layers formed on Ti6Al4V? (b) does the variation in HCO_3^- concentration affect the apatite-inducing ability of SBFs? and (c) how would the *in vitro* tests with mouse osteoblast discriminate between CaP coatings of different SBFs?

EXPERIMENTAL PROCEDURE

Ti6Al4V strips (Grade 5, McMaster-Carr), with the dimensions of 10 x 10 x 1 mm, were used as substrates. The strips were first abraded with a #1000 SiC paper (FEPA P#1000, Struers), and then washed three times, respectively with acetone, ethanol, and deionized water in an ultrasonic bath. Each one of such strips was then immersed in 50 mL of a 5M NaOH solution at 60°C for 24 hours in a glass bottle, followed by washing with deionized water and drying at 40°C.

Details of SBF preparation routines are given in Table II. Freshly prepared, 1.5x *c*-SBF [1], *Tas*-SBF [12], and *r*-SBF [10] solutions were used in coating experiments.

Table II 1.5 x SBF preparation

Order	Reagent	Weight (*g per L*)		
		c-SBF[1]	*Tas*-SBF[12]	*r*-SBF[1, 10]
1	NaCl	12.0540	9.8184	8.1045
2	$NaHCO_3$	0.5280	3.4023	1.1100
3	Na_2CO_3	—	—	3.0690
4	KCl	0.3375	0.5591	0.3375
5	$K_2HPO_4.3H_2O$	0.3450	—	0.3450
6	Na_2HPO_4	—	0.2129	—
7	$MgCl_2.6H_2O$	0.4665	0.4574	0.4665
8	1 M HCl	15 mL	15 mL	—
9	HEPES	—	—	17.8920
10	$CaCl_2.2H_2O$	0.5822	0.5513	0.5822
11	Na_2SO_4	0.108	0.1065	0.1080
12	TRIS	9.0945	9.0855	—
13	1 M HCl	50 mL	50 mL	—
14	1 M NaOH	—	—	0.8 mL

NaOH-treated Ti6Al4V strips were soaked at 37°C in 50 mL of 1.5x *c*-SBF, *Tas*-SBF and *r*-SBF in tightly sealed Pyrex® bottles of 100 mL-capacity, for a period of 7, 14 and 21 days. All the SBF solutions were replenished at every 48 hours. Strips were removed from the SBF solutions at the end of respective soaking times, and washed with deionized water, followed by drying at 37°C. The strips were placed either "horizontally" on the base of the immersion bottles or dipped "vertically" into the solutions with a stainless steel wire. Coated strips were examined by using an X-ray diffractometer (XDS 2000, Scintag Corp., Sunnyvale, CA), operated at 40 kV and 30 mA with monochromated Cu K_α radiation. X-ray data were collected at 2θ values from 4° to 40° at a rate of 0.01° per minute. FTIR analyses were performed directly on the coated strips (Nicolet 550, Thermo-Nicolet, Woburn, MA). Surface morphology of the sputter-coated (w/Pt) strips was evaluated with a scanning electron microscope (FE-SEM; S-4700, Hitachi Corp., Tokyo, Japan).

Mouse osteoblast cells, designated 7F2 (ATCC, Rockville, MD), were used for cell attachment studies on the SBF-coated strips. Cells were first grown at 37°C and 5% CO_2 in alpha MEM, augmented by 10% FBS. The culture medium was changed every other day until the cells reached a confluence of 90-95%. Osteoblasts were seeded at a density of 10^5 cells/cm^2. Cell cytotoxicity measurements were carried out after 24 hours, cell viability assessment was performed after 72 hours and total protein amount were measured after 7 days. Adhesion of the cells was quantified 24 hours after seeding. Trypan blue was added and the cells were counted using an Olympus BX60 light microscope. Only cells that stain blue were deemed necrotic because of plasma membrane damage. For statistics, all experiments were performed in triplicate where n=3. Analysis of variance was performed using the Tukey-Kramer multiple comparisons test. Osteoblast morphology after attachment was further examined using SEM. Prior to SEM investigations, samples were soaked in the primary fixative of 3.5% glutaraldehyde. Further, the cells were dehydrated with increasing concentrations of ethanol (50%, 75%, 90% and 100%) for

10 minutes each. Critical drying was performed according to the previously published procedures [20]. Samples were sputter-coated with Pt prior to the SEM imaging at 5 kV.

RESULTS AND DISCUSSION

During our preliminary studies, we also prepared 1xSBF solutions (i.e., *c*-, *r*-, and *Tas*-SBF) and tested the formation of calcium phosphates (CaP) on alkali-treated Ti6Al4V strips for 1 week of soaking at 37°C. There was almost no coating observed, regardless of the replenishment rate with these 1xSBF solutions. For 1xSBF solutions, more than 3 weeks of soaking is required to observe only the onset of coating. To accelerate the coating process, 1.5xSBF solutions were then prepared.

Ti6Al4V strips were placed vertically (i.e., the strips placed at the halfway point along the entire height of the solution level) in the 1.5xSBF-immersion bottles. Vertical placement of the strips produced a uniform, precipitate-free coating on the surfaces, in all three SBF solutions tested. Vertically-placed strips were also coated on both sides. SEM micrographs given in Figures 1(a) through 1(c) showed the uniform CaP coatings obtained.

c-SBF solutions with 4.2 mM HCO_3^- yielded a thin layer of calcium phosphate (CaP) coating, Fig. 1(a), in comparison to *Tas*-SBF solutions, Fig. 1(b). The nano-morphology difference between the CaP coatings of *Tas*- and *r*-SBF solutions was quite significant, Figs. 1(b) and 1(c). Tris-solutions always produced round globules consisting of 'needle-like, intermingling, interlocking nanosize calcium phosphates, whereas Hepes-solutions produced spherical aggregates on Ti6Al4V strips.

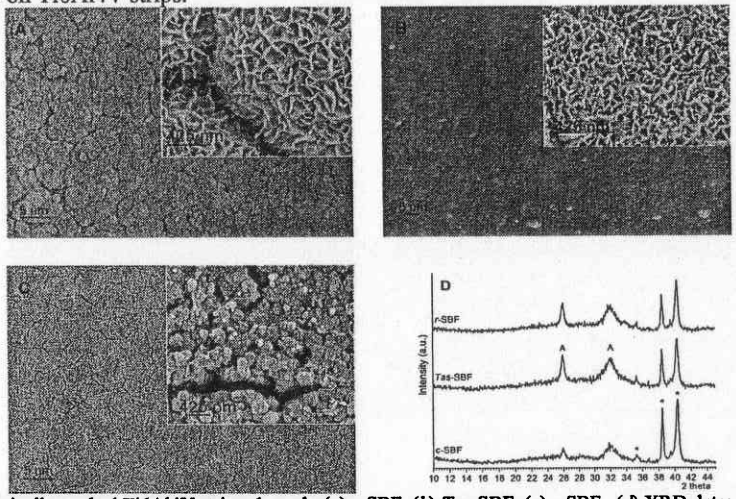

Fig. 1 Vertically-soaked Ti6Al4V strips, 1 week; (*a*) *c*-SBF, (*b*) *Tas*-SBF, (*c*) *r*-SBF, (*d*) XRD data; A denoted peaks of apatitic CaP, * Ti6Al4V peaks

XRD traces of the vertically-placed, 1 week-coated Ti6Al4V strips are given in Figure 1(d). *c*-SBF solutions still formed a lesser quantity of apatitic CaP on the strips as compared to those formed by the *Tas*- and *r*-SBF. These data clearly showed that (a) the carbonate ion concentration in 1.5xSBF solutions of pH 7.4 must be raised to the level of human blood plasma, i.e., 27 mM, to form a coating layer which fully covers the available strip surface in about 1 week, (b) the geometrical placement of the samples in SBF solutions has a strong effect on the

morphology of the coatings, and (c) nano-morphology of the coatings obtained in HEPES-buffered *r*-SBF solutions were significantly different than those obtained in TRIS-buffered *c*- and *Tas*-SBF solutions. The initial progress of the SBF-coating, as a function of soaking time, on vertically-placed Ti6Al4V strips was also studied. SEM micrographs of Figures 2(a) to 2(d) demonstrated the morphology differences between the CaP coatings of *Tas*- and *r*-SBF solutions, both having 27 mM HCO_3^-, after 2 and 4 days of soaking. FTIR data of the 3 weeks-soaked samples showed that all the coatings were consisted of carbonated (CO_3^{2-} ion absorption bands seen at 1470-1420 and 875 cm^{-1}) calcium phosphates, Figure 2(e). The absence of the stretching and the vibrational modes of the O-H group at 3571 and 639 cm^{-1} confirmed [21] that these coatings cannot simply be named as "hydroxylapatite." From the FTIR data alone, it is rather difficult to distinguish between the coatings of different SBF solutions.

The degree of supersaturation for carbonated apatite plays a major role in determining the coating behavior of a SBF solution and is directly proportional to the activity of the individual ion as calculated out by Lu et al. [22]. Under ideal solution conditions, the activity of the individual ion is equal to its concentration in the solution. Thus increasing the concentration of the individual ion will increase the activity and thus, increase the level of supersaturation. Another parameter affecting the behavior of coating is the ionic strength. *c*- and *Tas*-SBF have the same ionic strength values i.e., 160.5 mM, whereas *r*-SBF has a significantly lower value of 149.5 mM. Theoretically, if a solution has a low ionic strength, this means that the ionic diffusion will be enhanced in such a solution. Thus, in a solution with low ionic strength and high ionic diffusion, there will be more nucleation sites for the precipitation reactions, which will follow. CO_2 release from an aqueous solution will also be faster in a low ionic strength solution.

Mouse osteoblasts showed significant differences in terms of the number of attached cells, cell viability, and protein concentration, as presented in Figures 2(f) through 2(h), between the apatitic calcium phosphate layers obtained by using the SBF solutions of this study. The number of attached cells, %viability, and protein concentration were all found to yield the highest values in the case of using a 27 mM HCO_3^--containing, TRIS-HCl buffered SBF solution (i.e., *Tas*-SBF).

Osteoblast attachment on the surfaces of the SBF-coatings (on 3 weeks-soaked samples) was monitored by SEM, and given in Figures 3(a) through 3(f). Osteoblast behavior is sensitive to biochemical and topographical features (i.e., microarchitecture) of their substrate. The ideal and most preferred surface used by osteoblasts *in vivo* is the osteoclast resorption pit [23]. However, one may speculate that the surfaces of nanoporous, apatitic CaP coatings formed in an SBF solution at 37°C and pH 7.4 represents the next-to-the-best 'bioceramic' substrate for the osteoblasts to respond to. The cytotoxicity, % viability and the protein content histograms given in Figures 2(f) to 2(h) showed that the CaP-coated (in *Tas*-SBF) Ti6Al4V strips always performed better than either bare Ti6Al4V or NaOH-treated TiAl4V strips. Mouse osteoblasts were able to differentiate between CaP coatings of different SBF solutions. It was quite osteoblasts to respond to. The cytotoxicity, % viability and the protein content histograms given in Figures 2(f) to 2(h) showed that the CaP-coated (in *Tas*-SBF) Ti6Al4V strips always performed better than either bare Ti6Al4V or NaOH-treated TiAl4V strips. Mouse osteoblasts were able to differentiate between CaP coatings of different SBF solutions. It was quite interesting to note in Figure 2(h) that the adsorbed protein concentration measured in 7-days soaked samples of *Tas*-SBF was even higher than those of 21-days soaked in *c*-SBF solution. It is a well-known fact that the surface chemistry of a material determines the initial *in vitro*

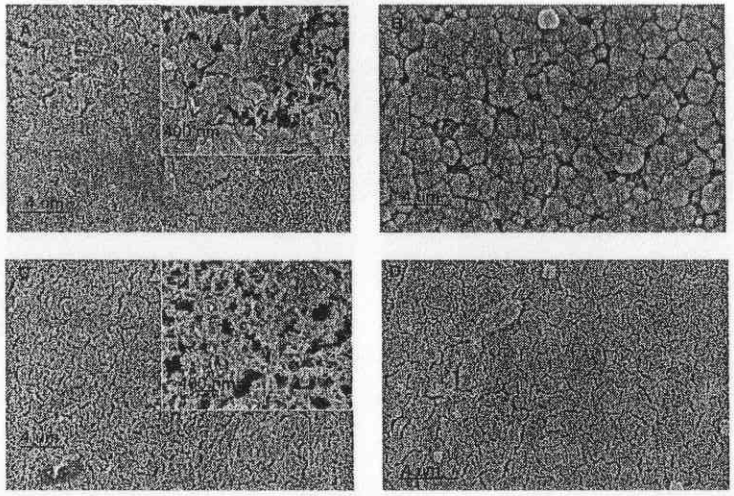

Fig. 2 (*a*) 2 days in *Tas*-SBF, (*b*) 4 days in *Tas*-SBF, (*c*) 2 days in *r*-SBF, (*d*) 4 days in *r*-SBF

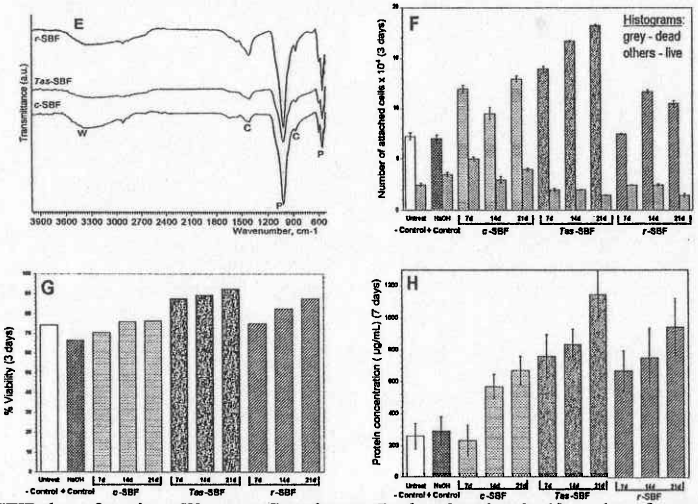

Fig. 2 (*e*) FTIR data of coatings; W: water, C: carbonate, P: phosphate bands, (*f*) number of osteoblasts attached on the CaP coatings of different SBFs after 3 d, (*g*) cell viability for *c*-, *Tas*- and *r*-SBF coatings after 3 d, (*h*) protein concentrations for different SBFs after 7 d.

interactions of proteins, such as fibronectin with integrin cell-binding domains, which in turn regulate the cell adhesion process. On coating surfaces, cells were flattened and spread with clear actin fibers associated with vinculin adhesion plaques (Fig. 3). The SEM micrograph of Fig. 3(d), recorded on a *Tas*-SBF-coated Ti6Al4V surface, clearly showed the actin cytoskeleton and the stress fibers. Micrographs of 3(b) and 3(f) displayed the vinculin adhesion plaque formation

on samples produced by using *c*-SBF and *r*-SBF, respectively. Cells are seen to produce fewer adhesion plaques while still in the process of migration than once permanently settled in place. Sun *et al.* [24] exposed cells to calcium phosphate particles and reported that HA particles (100 nm) or β-TCP particles (100 nm) inhibited the growth of primary rat osteoblasts, while causing an increase in their expression of alkaline phosphatase. In addition, Pioletti *et al.* [25] observed a decrease in growth, viability, and synthesis of extracellular matrix in primary rat osteoblasts that were exposed to β-TCP particles (1–10 μm) or $CaHPO_4 \cdot 2H_2O$ particles (1–10 μm). The absence of such effects in our case proved the biocompatible nature of the SBF-coatings studied. Figures 3(a), 3(c) and 3(e) revealed the extension of osteoblast filopodia.

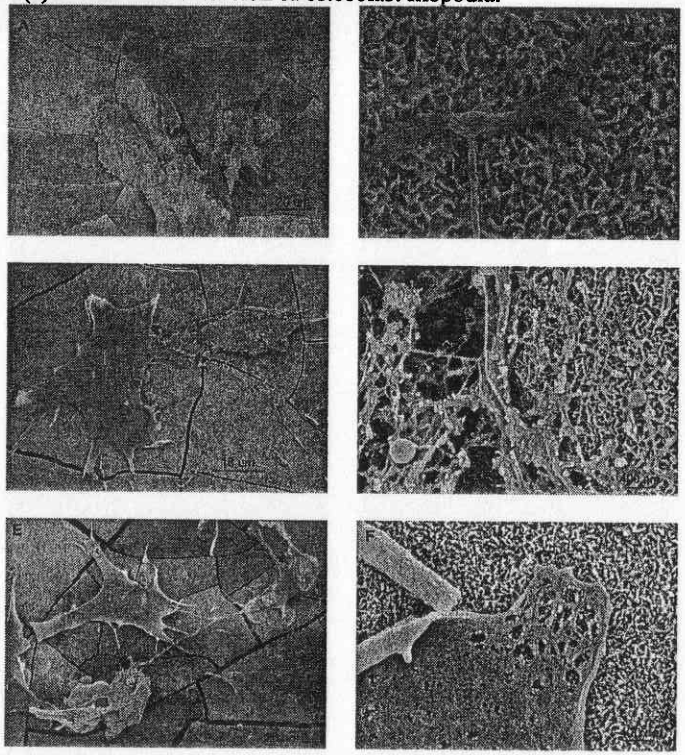

Fig. 3 SEM micrographs for the osteoblast attachment/adhesion on CaP coatings (3 weeks of soaking time) of different SBF solutions, (*a*) – (*b*): *c*-SBF, (*c*) – (*d*): *Tas*-SBF, (*e*) – (*f*): *r*-SBF.

CONCLUSIONS

This study enabled the direct comparison of HEPES and TRIS-buffered SBF solutions with one another, as well as with those of different HCO_3^- concentration and supersaturation levels. Apatite-inducing ability of NaOH-treated Ti6Al4V strips were compared when these strips were soaked at 37°C, from 2 days to 3 weeks, in three different SBF solutions, namely, *c*-SBF, *r*-SBF, and *Tas*-SBF. Although *r*-SBF and *Tas*-SBF both match the HCO_3^- concentration of human blood plasma, i.e., 27 mM, the former was buffered with HEPES, while the latter with

TRIS. The findings are: 1) There is a significant difference in coating morphology between the *r*- and *Tas*-SBF solutions both of 27 mM HCO_3^-. *r*-SBF formed more solution precipitates in comparison to TRIS-buffered SBF solutions (*Tas*-SBF); that would limit its long term use in coating substrates. 2) The nominal HCO_3^- concentration of an SBF solution is of crucial importance; an SBF solution containing 4.2 mM HCO_3^- can not contend in coating Ti6Al4V surfaces with an SBF solution of 27 mM HCO_3^-. The apatitic CaP formation rate of *c*-SBF on NaOH-treated Ti6Al4V was inferior to that of *Tas*-SBF. 3) SBF-coating process was considerably affected by the placement geometry of substrates in the SBF solutions; horizontally-placed substrates exhibited a growth pattern extending upwards in the solution, while the vertically-soaked strips were coated uniformly. 4) *In vitro* tests with rat osteoblasts cultured on the apatitic CaP coatings of this study favored the TRIS-buffered, 27 mM SBF solutions in terms of osteoblast attachment, cell viability and protein concentrations.

REFERENCES

1. T. Kokubo, *J. Non-Cryst. Solids* **120** (1990) 138.
2. T. Kokubo, *Acta Mater.* **46** (1998) 2519.
3. T. Kokubo, H.-M. Kim, M. Kawashita and T. Nakamura, *J. Mater. Sci. Mater. M.* **15** (2004) 99.
4. W. Earle, *J. N. C. I.* **4** (1943) 165.
5. J. H. Hanks and R. E. Wallace, *Proc. Soc. Exp. Biol. Med.* **71** (1949) 196.
6. S. Ringer, *J. Physiol.* **4** (1880-1882) 29.
7. L. Frauchiger, M. Taborelli, B. O. Aronsson and P. Descouts, *Appl. Surf. Sci.* **143** (1999) 67.
8. H.-M. Kim, H. Takadama, F. Miyaji, T. Kokubo, S. Nishiguchi and T. Nakamura, *J. Mater. Sci. Mater. M.* **11** (2000) 555.
9. A. Bigi, E. Boanini, S. Panzavolta and N. Roveri, *Biomacromolecules* **1** (2000) 752.
10. A. Oyane, K. Onuma, A. Ito, H.-M. Kim, T. Kokubo and T. Nakamura, *J. Biomed. Mater. Res.* **64A** (2003) 339.
11. A. P. Serro and B. Saramago, *Biomaterials* **24** (2003) 4749.
12. D. Bayraktar and A. C. Tas, *J. Eur. Ceram. Soc.* **19** (1999) 2573.
13. A. C. Tas, *Biomaterials* **21** (2000) 1429.
14. H.-M. Kim, T. Kokubo, J. Tanaka and T. Nakamura, *J. Mater. Sci. Mater. M.* **11** (2000) 421.
15. H. Eagle, *Science* **122** (1955) 501.
16. R. Dulbecco and M. Vogt, *J. Exp. Med.* **106** (1957) 167.
17. E. I. Dorozhkina and S. V. Dorozhkin, *Coll. Surface. A*, **210** (2002) 41.
18. L. Grondahl, F. Cardona, K. Chiem, E. Wentrup-Byrne and T. Bostrom, *J. Mater. Sci. Mater. M.* **14** (2003) 503.
19. P. A. A. P. Marques, M. C. F. Magalhaes and R. N. Correia, *Biomaterials* **24** (2003) 1541.
20. T. J. Webster, R. W. Siegel and R. Bizios, *Biomaterials* **20** (1999) 1221.
21. C. K. Loong, C. Rey, L. T. Kuhn, C. Combes, and M. J. Glimcher, *Bone*, **26** (2000) 599.
22. Xiong Lu and Yang Leng, *Biomaterials* **26** (2005) 1097.
23. B. D. Boyan, Z. Schwartz, C. H. Lohmann, V. L. Sylvia, D. L. Cochran, D. D. D. Dean and J. E. Puzas, *J. Orthop. Res.* **4** (2003) 638.
24. J. S. Sun, Y. H. Tsuang, C. J. Liao, H. C. Liu, Y. S. Hang and F. H. Lin, *J. Biomed. Mater. Res.* **37** (1997) 324.
25. D. P. Pioletti, H. Takei, T. Lin, P. V. Landuyt, Q. J. Ma, S. Y. Kwon and K. L. P. Sung, *Biomaterials* **21** (2000) 1103.